Photoionization of potassium atoms from the ground and excited states

O. Zatsarinny[1,*] and S. S. Tayal[2]

[1]*Department of Physics and Astronomy, Drake University, Des Moines, Iowa 50311, USA*
[2]*Department of Physics, Clark Atlanta University, Atlanta, Georgia 30314, USA*

The Dirac-based B-spline R-matrix method is used to investigate the photoionization of atomic potassium from the $4s$ ground and $4p$, $5s$-$7s$, $3d$-$5d$ excited states. The effect of the core polarization by the outer electron is included through the polarized pseudostates. Besides the dipole core polarization, we also found a noticeable influence of the quadrupole core polarization. We obtained excellent agreement with experiment for cross sections of the $4s$ photoionization, including accurate description of the near-threshold Cooper-Seaton minimum. We also obtained close agreement with experiment for the $4p$ photoionization, but there are unexpectedly large discrepancies with available experimental data for photoionization of the $5d$ and $7s$ excited states.

I. INTRODUCTION

Photoionization of atoms is the main elementary process in the interaction of electromagnetic radiation with matter, and the relevant photoionization cross sections have great significance in many applications such as astrophysics, plasma physics, atmospheric science, and the lighting industry. Despite a long history of their measurements and calculations, the photoionization cross sections for many atoms remain mostly uncertain. It is particularly intriguing in the case of alkali-metal atoms, which can be regarded among the simplest atoms for theory. Alkali-metal atoms as quasi-one-electron systems have proven to be a valuable and interesting testing ground for theoretical description of the photoionization process, both for *ab initio* theories and semiempirical calculations. In particular, photoionization of alkali-metal atoms in their ground state has received a lot of attention due to the Cooper-Seaton minimum appearing close to threshold which provides a sensitive probe of electron correlation and relativistic effects.

In order to achieve confidence in theoretical values of cross sections and to obtain good understanding of atomic interactions, comparison with experiment is essential to benchmark theory. The accuracy of experimental data for photoionization of alkali-metal atoms, however, is limited by uncertainty in the density calibration and systematic effects due to alkali-metal molecules. These molecules are always present along with alkali-metal atoms and their cross sections are not known well. The above difficulties are partly responsible that the available experimental cross sections [1,2] for photoionization of neutral potassium differ by up to a factor of 2 and therefore cannot serve as benchmark data for testing of theories. More recently, Sander *et al.* [3] carried out additional measurements for a more detailed study of the Cooper-Seaton minimum. Their cross sections at the minimum are considerably lower than obtained in previous measurements [1,2]. The available theoretical calculations [4–8] for photoionization of potassium differ considerably from each other and these differences do not allow any one favorite among the experimental data mentioned above. Usually calculated cross sections were

compared with one experiment, ignoring the other experimental data. In particular, no one theory reproduces accurately enough the experimentally observed near-threshold minimum where short-range correlation and relativistic effects are very important.

Photoionization of many-electron atomic systems from the excited states provides a deeper understanding of complex interactions and dynamical effects. The measurements of photoionization cross sections from excited states are based on resonance ionization of atoms and molecules as a result of successive absorption of several laser photons. Nygaard *et al.* [9] pioneered the measurements of the photoionization cross section of potassium from the $4p$ excited state using the two-step photoionization process. Later, Petrov *et al.* [10] reported absolute $4p_{3/2}$ photoionization cross section of potassium at three selected photoelectron energies. They also presented the partial and total photoionization cross sections of potassium using configuration interaction technique and discussed the effect of polarization of the atomic core by the valence electron. More recently, Amin *et al.* [11] reported new measurements of the photoionization cross sections from the $4p_{1/2,3/2}$, $5d_{3/2,5/2}$, and $7s_{1/2}$ excited states of potassium. Their photoionization cross sections from the $4p_{3/2}$ state are in good agreement with the other measured values, whereas the photoionization cross sections from the $5d$ and $7s$ excited states were reported for the first time. These recent measurements of the photoionization cross sections from the $4p$, $5d$, and $7s$ excited states of potassium provide an opportunity to test the theory and where no earlier theoretical data are available for comparison.

The theory of the atomic photoionization has been fully developed during the past 4 decades. The accuracy of a particular calculation, however, critically depends on the method and the model chosen for the calculation. The many-electron systems cannot be described exactly, so the success of a calculation depends on how much correlation effects can be incorporated in a given method. It is well known that the most important correlation effects in alkali-metal atoms are connected with the core polarization. The core polarization most simply can be included with a semiempirical model potential, as has been done by Weistheit [4]. The comparison of his results with measurements [1] shows a good agreement in the energy region from the threshold to the cross-section minimum, but at

---

*oleg.zatsarinny@drake.edu

higher photoelectron energies the measured cross section rises much more steeply than the computed cross section does. The semiempirical approach is simple in implementation, but the complete inclusion of different correlation effects in the model potential may be questionable.

One of the first calculations of the photoionization of potassium from the first principle was undertaken by Saha [6]. The effects of core polarization were taken into account by using extensive multiconfiguration expansions both for the initial $3p^6 4s$ bound state and for the final $3p^6 kp$ continuum states. However, it is not clear that how much core polarization has been taken into account in this calculation. Saha obtained good agreement with experimental data of Hudson and Carter [1] except for higher energies above 5 eV. Another attempt to consider the core-polarization potential in *ab initio* calculations has been undertaken by Petrov *et al.* [7]. The core polarization potential has been derived numerically by applying the variational principle to the total energy of atom. The calculated potential was found considerably deeper inside the atomic core than the previously used model core potential in the work of Weistheit [4]. The photoionization cross section obtained in this approach is in very good agreement with the experimental data of Marr and Creek [2]. Thus the two most extensive calculations performed from the first principle closely agree with different measurements which, however, disagree with each other by up to a factor of 2 at higher energies.

The present calculations were motivated partly by the diversity of the existing theoretical and experimental data as outlined above. In this article we reexamine the $h\nu + $ K problem using the fully relativistic version of the *B*-spline *R*-matrix (BSR) method. The BSR complex [12] has been extensively used for studies of low-energy electron-atom and photon-atom scattering for the past 10 years, and its relativistic extension called Dirac *B*-spline *R*-matrix (DBSR) method was introduced only recently in our investigations of the electron scattering on Cs [13] and Hg [14]. In all our previous studies we incorporated the core-valence correlation through the core-excited states in the close-coupling expansion that usually leads to a very extensive calculation. In this paper we present the further extension of the DBSR complex by introducing polarized pseudostates as a complete and computationally very efficient way to incorporate the core-valence correlation. The polarized states also allow us to include higher multipoles.

This article is organized as follows. In Sec. II we outline the present theoretical method with details of the polarized pseudostates and photoionization cross sections in the *B*-spline basis. Results for photoionization of the 4*s* ground state and the 4*p*, 5*s*-7*s*, 3*d*-5*d* excited states of potassium are presented and discussed in Sec. III. In Sec. IV we conclude with a brief summary. Unless specified otherwise, atomic units are used throughout the article.

II. COMPUTATIONAL MODEL

All calculations reported in this article were performed in the fully relativistic approach based on the Dirac-Coulomb Hamiltonian

$$H_{\text{DCB}} = \sum_i h_D(r_i) + \sum_{i<j} \frac{1}{r_{ij}}, \tag{1}$$

$$h_D = c\alpha \mathbf{p} + \beta c^2 + V_{\text{nuc}}(r), \tag{2}$$

where all quantities have their usual meaning. Specifically, we employed our newly developed Dirac *B*-spline *R*-matrix complex which is an extension of the BSR complex [12] to the fully relativistic Dirac scheme. It was described in detail in recent applications to *e*-Cs [13] and *e*-Hg [14] collisions. The distinguishing features of the method are: (i) the ability to use term-dependent and hence nonorthogonal sets of one-electron Dirac spinors in the target description and (ii) *B* splines as the underlying, effectively complete, basis to expand the one-electron radial functions. Furthermore, it is an *all electron approach* and hence different correlation effects such as the core polarization can be described *ab initio* using the many-electron configuration expansions. The total wave functions was constructed from four-component Dirac spinors

$$\phi_{n\kappa m}(\mathbf{r}) = \frac{1}{r} \begin{pmatrix} P_{n\kappa}(r)\chi_{\kappa m}(\hat{r}) \\ i\, Q_{n\kappa}(r)\chi_{-\kappa m}(\hat{r}) \end{pmatrix}; \tag{3}$$

and in the present method the radial functions for the large and small components $P(r)$ and $Q(r)$ were expanded in individual *B*-spline bases of different order as

$$P(r) = \sum_{i=1}^{n_p} p_i B_i^{k_p}(r); \quad P(r) = \sum_{i=1}^{n_q} q_i B_i^{k_q}(r). \tag{4}$$

Using different orders for large and small components allowed us to avoid the occurrence of unphysical pseudostates as discussed by Froese Fischer and Zatsarinny [15]. In the present calculations we used a semiexponential grid for the *B*-spline knot sequence and a relatively large number of splines (115) to cover the region up to the *R*-matrix radius of $80 a_0$, where a_0 denotes the Bohr radius.

We begin by describing the structure model used for the K target. This is followed by a summary of the photoionization calculation.

A. Structure calculations

All atomic states considered in the present calculations have simple quasi-one-electron structure (core)*nlj* or (core)*klj* for initial bound or final continuum states, respectively. The core has configuration $K^+(1s^2 2s^2 2p^6 3s^2 3p^6)$ and we started by generating the core orbitals from a K^+ Dirac-Fock (DF) calculation using the GRASP2K relativistic atomic-structure package [16]. In order to elucidate the importance of inner-core correlation, we considered two models for the core wave functions: the one-configuration approximation and the many-configuration approximation, which includes all configurations obtained from single and double promotion of the 3*s* and 3*p* orbitals into the four *l*-correlated orbitals, optimized for the $(3s^2 3p^6)$ ground state of K^+. In the final core expansion we retained all configurations with expansion coefficients $c > 0.01$.

The main correlation effects in the K atomic states are related with the core-valence interaction. In most previous calculations for alkali-metal atoms, a phenomenological one-electron core polarization potential was usually added to account for the core-valence correlation. Although such a potential simplifies the calculations significantly and can

provide accurate excitation energies and oscillator strengths, the question always remains how well the model potential can simulate whole core-valence correlation, including nondipole contributions. The core-valence correlation can also be included *ab initio* by adding target states with an excited core. Such an approach was applied, for example, by Saha [6] for the $h\nu + K$ problem and in our recent calculations for $e + Cs$ scattering [13]. This is the most consistent approach, but it leads to very large close-coupling expansions and extensive computational efforts. Besides, in case of the $3p^6$ core, typically 50% or more of the core polarizability comes from the continuum that is very difficult to incorporate into close-coupling expansions. One solution to this problem in the case of electron-hydrogen scattering was given by Damburg and Karule [17]. They pointed out that it was possible to define a pseudostate which could be included in the close-coupling expansion in the same way as an atomic eigenstate but which allowed for the full polarizability of the ground state. We will refer to this state as a polarized pseudostate to distinguish it from pseudostates which have been widely used to represent other aspects of the collision process. For example, in the *R*-matrix pseudostate (RMPS; [18]) or convergent close-coupling (CCC; [19]) methods, pseudostates are used to mimic the target continuum and they are usually determined from diagonalization of the atomic Hamiltonian in the bases of L^2 integrable wave functions.

First attempt to employ polarized pseudostates in scattering problem was made by Burke and Mitchell [20], who obtained the polarized pseudostates as linear combination of configurations based on analytic orbitals. Further development of using polarized pseudostates in the multiconfigurational approach for calculation of atomic polarizabilities has been reported in a series of articles by Hibbert *et al.* [21]. In the present calculations we follow these developments but employ the different numerical technique which is based on the *B*-spline expansions.

The polarized pseudostate ϕ_p is defined by the requirement that the static polarizability of atomic state ϕ_0 can be expressed by a single term

$$\alpha = 2\frac{|\langle\phi_0|\mathbf{D}^{(1)}|\phi_p\rangle|^2}{E_p - E_0}, \tag{5}$$

where $\mathbf{D}^{(1)}$ is a dipole operator and ϕ_p is a normalized solution of the atomic Hamiltonian, that is,

$$\langle\phi_p|\phi_p\rangle = 1 \tag{6}$$

and E_p is defined by

$$\langle\phi_p|H|\phi_p\rangle = E_p. \tag{7}$$

As shown by Burke and Mitchell [20], the ϕ_p can be written as

$$\phi_p = N^{-1/2}\tilde{\phi}_p, \tag{8}$$

where $\tilde{\phi}_p$ is a solution of the equation

$$(H - E_o)\tilde{\phi}_p = D_0^{(1)}\phi_0 \tag{9}$$

and the factor $N^{-1/2}$ ensures that Eq. (6) is satisfied. The generalization to any higher multipole k is straightforward by using multipole operator $\mathbf{D}^{(k)}$.

In the present calculations of the core polarization, we take into account the excitations from both the $3s^2$ and $3p^6$ subshells, so that the expansions for the polarized pseudostate have the form

$$\phi_p^{(k)} = A[\Phi(3s^23p^5)\phi_1(l_1j_1)]^{J\pi} + A[\Phi(3s3p^6)\phi_2(l_2j_2)]^{J\pi} \tag{10}$$

where A denotes the antisymmetrization operator and we consider all possible channels. Because the core has $J_0 = 0$, the total moment J for polarized pseudostates equal to multipole index k. The unknown large and small radial components for the pseudo-orbitals $\phi_i(l_ij_i)$ in Eq. (10) were expanded in the *B*-spline basis as shown in Eq. (4). The coefficients of the *B*-spline expansions, p_i and q_i, were found from the inhomogeneous Eq. (9). In the *B*-spline basis, this equation has the form

$$(\mathbf{H} - E_0\mathbf{S})\mathbf{c} = \mathbf{D}\mathbf{c}_0, \tag{11}$$

where $\mathbf{H}$, $\mathbf{S}$, and $\mathbf{D}$ are the Hamiltonian, overlap, and dipole matrices between the basis functions for the (N-1)-electron system of K^+, and $\mathbf{c}$ and $\mathbf{c}_0$ are the vectors of *B*-spline expansions for the polarized pseudostates and the initial $K^+(3p^6)$ bound state, respectively.

The calculated multipole polarizabilities for the $K^+(3p^6)$ core are compared in Table I with other calculations and experiment. Our dipole polarizability obtained with multiconfigurational core expansion agree well both with experiment and other calculations, though calculations with HF core differ by $\sim$20%. It is a clear indication of the importance of the inner-core correlation for the $K^+(3p^6)$ core. The inner-core correlation effects also provide noticeable corrections ($\sim$10%) due to the quadrupole and octupole polarizabilities.

The polarized states of K^+ with multipole indexes $k = 1, 2, 3$ together with the ground-state $K^+(3p^6)$ were then used as target states in the *B*-spline bound-state close-coupling calculations to generate the low-lying states of atomic K. The corresponding close-coupling expansion has the structure

$$\Psi(3p^6nlj;J\pi) = A[\Phi(3s^23p^6)\phi(nlj)]^{J\pi}$$
$$+ A\sum_{k=1-3}\left[\phi_p^k\phi(n'l'j')\right]^{J\pi} \tag{12}$$

TABLE I. K^+ multipole polarizabilities (in atomic units).

	$\alpha^{(1)}$
5.47(5)	Spectral analysis [29]
5.46	RRPA [30]
5.52	RMBPT [31]
6.51	DBSR_DF, present result with DF core.
5.41	DBSR_CI, present results with CI core.
	$\alpha^{(2)}$
16.27	RRPA [30]
16.85	DBSR_DF
15.03	DBSR_CI
	$\alpha^{(3)}$
110	RMBPT [32]
109.6	DBSR_DF
100.9	DBSR_CI

The first term describe the physical states, whereas the other terms describe the core-polarization effects. The unknown large and small radial components for the outer valence electron, $\phi(nlj)$, were again expanded in individual B-spline bases. The coefficients of these expansions were found by diagonalizing the Dirac-Coulomb Hamiltonian given by Eq. (1) with the additional requirement that the wave functions vanish at the boundary. More specifically, using the B-spline basis leads to a generalized eigenvalue problem of the form

$$\mathbf{Hc} = E\mathbf{Sc}, \tag{13}$$

where again $\mathbf{H}$ and $\mathbf{S}$ are the Hamiltonian and overlap matrices between the basis functions. They are similar to matrices in Eq. (11) but now for N-electron system of atomic potassium. If orthogonality conditions are imposed between the scattering orbitals, $\mathbf{S}$ reduces to a banded matrix whose elements are the overlaps between individual B splines. In the general case of nonorthogonal orbital sets, however, it has a more complicated structure [12]. Note that we require orthogonality of $\phi(nlj)$ only to physical $3s$ and $3p$ orbitals but not to the correlated orbitals used for describing the inner-core correlation. The number of physical states which we can be obtained from Eq. (13) depends on the size of box. We choose box of radius $a = 80 \, a_0$ that allows us to obtain all bound states up to $9s$.

In order to illustrate the accuracy that can be achieved with polarized pseudostates in bound-state calculations, Table II compares the binding energies for potassium states up to $9s$ calculated with inclusion of the dipole-, quadrupole-, and octupole-polarized pseudostates. The correlation corrections in the binding energies are caused mainly by core-valence interaction and can be defined as difference between experimental values and one-configuration DF results. As seen from Table II, the ground state shows the biggest correlation correction and inclusion of the dipole polarization covers about 95% of the difference with experiment. The inclusion of the quadrupole- and octupole-polarized pseudostates further increases the binding energy, and final binding energy is slightly overestimated. It can be explained by the fact that polarized pseudostates describe mainly the long-range correlation related with single excitations of core. The above scheme does not include the double excitations of core which can be responsible for the remaining difference of 1–2%.

The binding energies for the $4p$ excited states show similar pattern but here the dipole polarization covers only 88% and the higher-order polarization is more important. The slowest convergence of binding energies were found for the nd states, whereas for the nf states the corrections are small and very well described by dipole polarization. The dipole polarization also dominates for higher-excited ns and np states, which are well described in the present scheme. The overall agreement is rather satisfactory taking into account that the present calculations are completely *ab initio* calculations and are made with relatively simple computational procedure.

B. Photoionization calculations

The photoionization calculations reported in this paper were performed using the R-matrix (close-coupling) approach. In the R-matrix method, the configuration space is partitioned into two regions separated by the R-matrix boundary

TABLE II. Binding energies (in eV) of potassium states with inclusion of the dipole ($k = 1$), quadrupole ($k = 2$), and octupole ($k = 3$) core polarization.

nl	j	NIST	DF	$k = 1$	$k = 2$	$k = 3$	Diff.
$4s$	1/2	4.341	4.013	4.321	4.340	4.347	−0.006
$4p$	1/2	2.731	2.604	2.716	2.730	2.734	−0.003
$4p$	3/2	2.724	2.599	2.709	2.723	2.727	−0.003
$5s$	1/2	1.734	1.662	1.727	1.733	1.735	0.001
$3d$	5/2	1.671	1.580	1.649	1.660	1.668	0.003
$3d$	3/2	1.670	1.580	1.648	1.659	1.668	0.003
$5p$	1/2	1.278	1.241	1.272	1.277	1.278	0.000
$5p$	3/2	1.276	1.239	1.270	1.275	1.275	0.000
$4d$	5/2	0.944	0.894	0.928	0.934	0.938	0.006
$4d$	3/2	0.944	0.893	0.927	0.933	0.938	0.006
$6s$	1/2	0.937	0.910	0.934	0.937	0.937	0.000
$4f$	5/2	0.853	0.850	0.854	0.854	0.854	0.000
$4f$	7/2	0.853	0.850	0.854	0.854	0.854	0.000
$6p$	1/2	0.745	0.729	0.743	0.745	0.745	0.000
$6p$	3/2	0.744	0.728	0.742	0.743	0.744	0.000
$5d$	5/2	0.598	0.570	0.588	0.591	0.594	0.004
$5d$	3/2	0.598	0.570	0.588	0.591	0.594	0.004
$7s$	1/2	0.587	0.574	0.586	0.587	0.587	0.000
$5f$	5/2	0.546	0.544	0.546	0.546	0.546	0.000
$5f$	5/2	0.546	0.544	0.546	0.546	0.546	0.000
$7p$	1/2	0.488	0.480	0.487	0.488	0.488	0.000
$7p$	3/2	0.488	0.480	0.486	0.487	0.488	0.000
$6d$	5/2	0.411	0.394	0.405	0.407	0.408	0.003
$6d$	3/2	0.411	0.394	0.405	0.406	0.408	0.003
$8s$	1/2	0.402	0.395	0.401	0.402	0.402	0.000
$6f$	5/2	0.379	0.378	0.379	0.379	0.379	0.000
$6f$	7/2	0.379	0.378	0.379	0.379	0.379	0.000
$8p$	1/2	0.345	0.340	0.344	0.345	0.345	0.000
$8p$	3/2	0.345	0.340	0.344	0.344	0.344	0.000
$7d$	5/2	0.299	0.288	0.295	0.296	0.297	0.002
$7d$	3/2	0.299	0.288	0.295	0.296	0.297	0.002
$9s$	1/2	0.293	0.288	0.292	0.293	0.293	0.000

at $r = a$. The latter is chosen in such a way that the magnitude of the radial spinors describing the bound electrons in the target is sufficiently small so that exchange between the incident electron and any target electron outside the R-matrix sphere is negligible. In the inner region, the total-scattering wave function is expanded in terms of an energy-independent basis set. In the present calculations, the R-matrix expansion and boundary radius a were chosen exactly the same as in the expansion (12) for bound states of atomic potassium. The only difference with bound-state calculations is the imposed boundary conditions. The R-matrix basis functions for the continuum electron are chosen to satisfy the boundary conditions [22]

$$\frac{Q_i(a)}{P_i(a)} = \frac{b + \kappa}{2ac}, \tag{14}$$

where b is an arbitrary constant usually chosen as 0. In practical calculations the boundary conditions in Eq. (14) can be imposed by adding the Bloch operator to the total Hamiltonian as was discussed in Refs. [13,15]. To find complete set of solutions in the inner region we should diagonalize the Hamiltonian in a given basis. In the B-spline representation

(4) for one-electron orbitals, this procedure again leads to eigenvalue problem (13) with **H** matrix modified by adding the Bloch operator. We see that in the B-spline basis both bound and continuum calculations are reduced to the calculations of matrix elements and solution of the matrix equations. Here we exploit the effective completeness of B-spline basis.

From the complete set of solutions in the inner region, an R-matrix relation can be derived that connects the solutions in the inner and outer regions. For a given energy E, this relation has the form

$$P_i(a) = \sum_j R_{ij}(E)[2acQ_j(a) - bP_j(a)], \quad (15)$$

where the relativistic R matrix is defined as

$$R_{ij}(E) = \frac{1}{2a} \sum_k \frac{P_{ik}(a)P_{jk}(a)}{E_k - E}. \quad (16)$$

Here the E_k are the R-matrix poles while the P_{ik} are the surface amplitudes of the basis function Ψ_k in channel i. Note that the surface amplitudes in the B-spline representation are simply defined by expansion coefficient of the last B spline, the only B spline which has nonzero value on the boundary.

The reactance matrix in the R-matrix method is defined by matching the external and internal solutions at $r = a$. In the external region, exchange between the scattered electron and the target electrons is neglected. Consequently, the channel wave functions satisfy a set of coupled differential equations described in detail by Young and Grant [23]. Except for very highly charged target, the scattered electron can be well described in a nonrelativistic framework. In the present calculations, therefore, we follow Norrington and Grant [22] and use the nonrelativistic limit of the Dirac radial equations for the scattered electron in the asymptotic region. Specifically, we use the program ASYPCK [24] for treating the external region. Note that in the outer region we have the n_0 independent solutions, where n_0 is the number of open channels which are defined by all target states accessible at a given excitation energy.

In the R-matrix theory, the photoionization cross sections can be defined through the dipole matrix between the initial state Ψ_o and the R-matrix basis states Ψ_k provided that all radial orbitals of the initial state are well confined in the inner region. The total photoionization cross section for a given photon energy ω is

$$\sigma(\omega) = \frac{8}{3}\pi^2 a_0^2 \alpha \omega^{\pm 1} \frac{1}{2J_0 + 1} \sum_j |(\Psi_j^- ||D||\Psi_o)|^2 \quad (17)$$

where D is a general dipole operator which could be either the length or velocity operator, and signs $(+1)$ and (-1) correspond to the length and velocity forms. Index j goes over different open channels, and other quantities have their usual meaning. Expanding Ψ_j^- in terms of the R-matrix states, we find that

$$(\Psi_j^- ||D||\Psi_o) = \frac{1}{a} \sum_k \frac{(\Psi_k ||D||\Psi_o)}{E_k - E_0 - \omega} \mathbf{P}_k^T \mathbf{R}^{-1} \mathbf{F}_j^-(a), \quad (18)$$

where $\mathbf{P}_k$ is the vector of the surface amplitudes (15), and $\mathbf{F}^-$ is constructed from the solutions in the outer region such that it satisfies the boundary condition

$$\mathbf{F}^- \rightarrow (\pi k)^{-1/2}(\sin\theta + \cos\theta\mathbf{K})(1 + i\mathbf{K})^{-1} \quad (19)$$

corresponding to a Coulomb modified plane wave plus an ingoing spherical wave.

III. RESULTS AND DISCUSSION

A. Photoionization of the ground state

We first discuss the convergence of the photoionization cross sections with respect to the inclusion of inner-core correlation and polarized pseudostates of different order. Figure 1 compares the ground state photoionization cross sections obtained with subsequent inclusion of the dipole, quadrupole, and octupole polarized states together with DF results without and with dipole core polarization. We see huge differences between the DF results and the DF cross sections with dipole core polarization that confirms the importance of the core polarization. The inclusion of inner-core correlation also leads to considerable reduction in cross sections at higher energies. Dipole core polarization provides the dominant contribution; however, the quadrupole interaction also has significant effect, up to 10% at higher photon energies. Octupole polarization contribution is only about 1–2%, so we may consider the cross sections to be converged. Our best results are calculated with inner-core correlation and with dipole, quadrupole, and octupole core polarization, and these are shown by a solid line in Fig. 1.

Figure 2 compares our best results with other calculations and experimental data. Our photoionization cross sections closely agree with the measurements of Marr and Creek
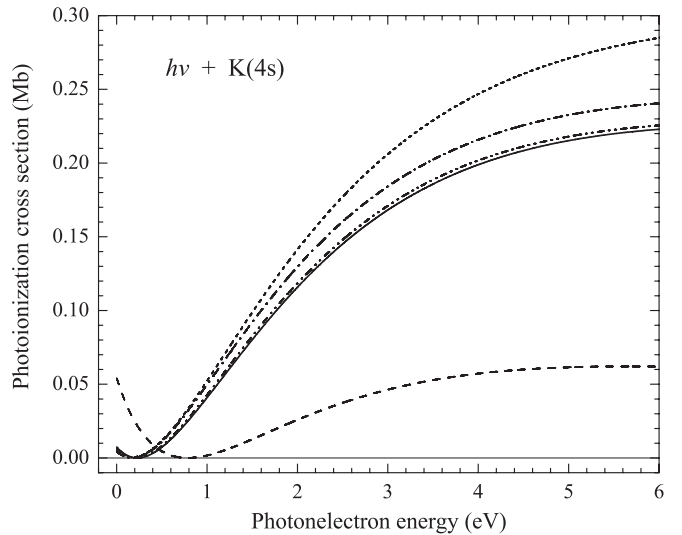
FIG. 1. Photoionization cross sections for the $4s$ ground state of K as a function of photoelectron energy. (Dashed line) Dirac-Fock (DF) calculation; (dotted line) DF with dipole core polarization; (dash-dotted line) DBSR calculation with dipole core polarization; (dash-double dotted line) DBSR calculation with dipole and quadrupole core polarization; (solid line) DBSR calculation with dipole, quadrupole, and octupole polarization.
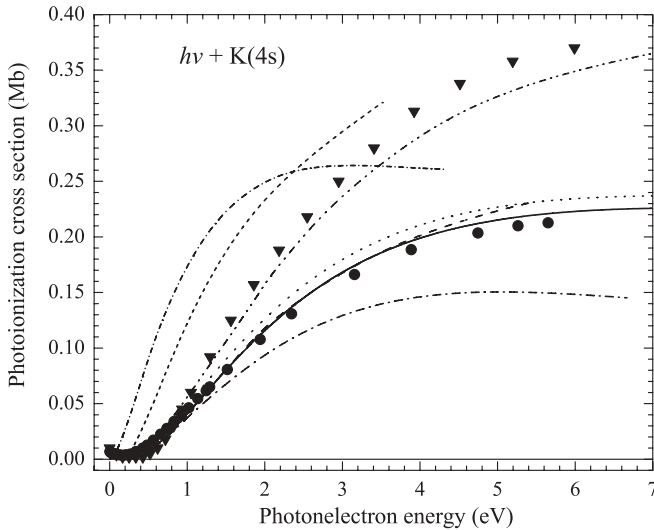
FIG. 2. Photoionization cross sections for the $4s$ ground state of K as a function of photoelectron energy. (Solid line) present length results; (dotted line) present velocity results; (large dashed line) calculated results of Petrov *et al.* [7]; (small dashed line) RMBPT calculation [8]; (large dash-dotted line) model potential calculation [4]; (small dash-dotted line) RRPA calculation [5]; (dash-double dotted line) MCHF calculation [6]; (solid circles) experimental data [2]; (solid triangles) experimental data [1].

[2] and are considerably lower than the measurements of Hudson and Carter [1] at higher energies. We present our cross sections in both length and velocity forms of dipole operator. The difference between these two forms is widely used as an estimation of the accuracy of the results. We see that our length and velocity cross sections differ by about 5%. The differences can be attributed to some short-range correlation effects which are not included in the present model and cannot be described within the polarized pseudostates method. Our results are compared with the semiempirical model-potential calculations of Weistheit [4]. This approach requires empirical parameters to describe the polarization potential. The adjustable parameters in Ref. [4] have been fitted to reproduce the correct position of the Cooper minimum at the threshold energies. As seen from Fig. 2, these calculations agree closely with the measurements at energies from the threshold through the region of the cross-section minimum, but at higher photoelectron energies the measured cross section rises much more steeply than the computed cross section does. Thus it may be concluded that the adjusted polarization potential used in Ref. [4] allows to describe only a part of correlation corrections which are required for accurate calculation of photoionization cross sections at lower energies.

One of the first attempts to set up a consistent *ab initio* relativistic many-body theory of photoionization including higher-order interactions between the core and valence electrons has been reported by Fink and Johnson [5]. They used the relativistic random-phase-approximation (RRPA) approach which includes the effects of the virtual excitation of the ionic core but ignores secondary effects of the valence electron on the core. As seen from Fig. 2, the results of the RRPA calculation show only qualitative agreement with experiment. They predict sharp rise in the cross section close to threshold

energies, therefore considerably improving the DF results, but RRPA cross sections are generally too high compared to the experimental values and the Cooper minimum is pushed slightly below threshold.

Further development of the relativistic many-body perturbation theory (RMBPT) for the calculations of photoionization cross sections has been reported recently by Savukov [8]. He explored the causes why otherwise highly accurate RMBPT methods when applied to bound-bound transition (see, e.g., Ref. [25]) reach much lower accuracy for alkali-metal atoms in calculations of photoionization cross sections, which are essentially proportional to squares of dipole matrix elements between bound and continuum states. Savukov introduced the quasicontinuum B-spline orbitals and additionally took into account all third-order terms. The noticeable improvement in results, especially in the near-threshold region, is clear from Fig. 2, but the RMBPT cross sections still considerably exceed the experimental values at intermediate energies.

Saha [6] calculated the photoionization cross sections of potassium using the multiconfigurational Hartree-Fock (MCHF) approach. The effects of core polarization were taken into account by including the configurations with single replacements of core orbitals, producing therefore dipole, quadrupole, and other multipole effects. This procedure is equivalent to the close-coupling calculation with inclusion of core-excited target states to some extent. The MCHF calculations, however, cannot answer how much core polarization has been taken into account and how quickly the close-coupling expansion will converge. Because considerable part of the $3p^6$ core polarization comes from the excitation to the continuum, we may assume that the differences between our calculation and the MCHF cross sections are due to slow convergence of close-coupling expansion for the $3p^6$ core. The MCHF calculation of Saha is the nonrelativistic calculation in LS coupling, and therefore it could not reproduce the nonzero Cooper minimum. Saha obtained good agreement with the experimental data of Hudson and Carter [1].

Petrov *et al.* [7] used the numerical core-polarization potential in their calculation which has been derived by applying the variational principle to the total energy of the atom written with the second-order correlation corrections. The calculated potential was found considerably deeper inside the atomic core than the previously used model core polarization potentials [4]. This potential has been then used in the framework of configuration interaction Pauli-Fock calculations to incorporate relativistic and other many-electron effects. The asymptotic behavior of the calculated potential has been compared with the well-known formula $\alpha_d r^{-4}$ to obtain dipole polarizabilities of the ionic core. Using the fitting factor of 1.25 for Slater integrals incorporated into their expression for polarization potential, they obtained $\alpha_d = 6.14$, 5.84, and 6.72 for $l = 0$, 1, 2, respectively. These values are somewhat larger than our values (see Table I). However, as seen from Fig. 2, their photoionization cross sections are very close to the present results for intermediate photoelectron energies from 1 to 4 eV but begin to diverge at higher energies.

Figure 3 compares the experimental and theoretical photoionization cross sections at the Cooper-Seaton minimum which appears in potassium very close to the threshold. The pronounced dip or minimum near threshold in the
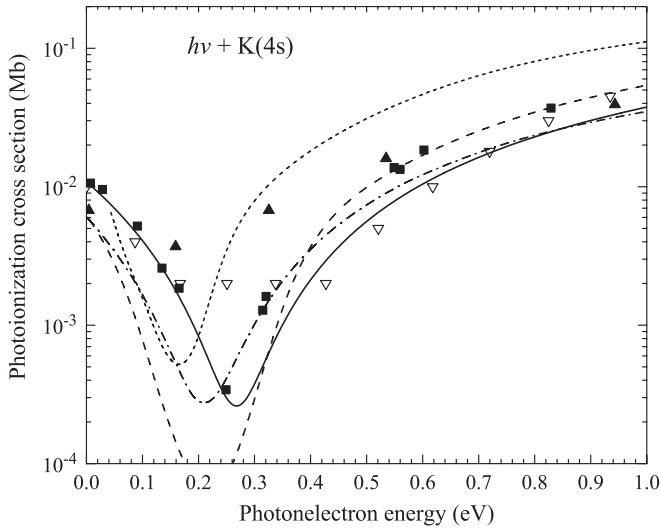
FIG. 3. Photoionization cross sections for the 4s ground state of K in the energy region of Cooper-Seaton minimum. (Solid line) present results; (dotted line) RMBPT calculation [8]; (dashed line) MCHF calculation [6]; (dash-dotted line) model potential calculation [4]; (solid rectangles) experimental data [3]; (solid triangles) experimental data [2]; (inverted triangles) experimental data [1].

FIG. 4. Photoionization cross sections for 4$p_{3/2}$ and 4$p_{1/2}$ excited levels of K as a function of photoelectron energy. (Solid line) Present results for the 4$p_{3/2}$ level; (dashed line) present results for the 4$p_{1/2}$ level; (dash-dotted line) calculation of Petrov *et al.* [7]; (dotted line) present DF calculation; (solid circles) experimental data of Petrov *et al.* [7]; (inverted solid triangles) experimental data for 4$p_{3/2}$ [11]; (upward solid triangles) experimental data for 4$p_{1/2}$ [11].

photoionization cross sections of Na, K, Rb, and Cs has been of interest for a long time [26]. The minimum occurs when the photoionization amplitude from the ground states as a function of photon energy passes through zero. There are two partial waves $p_{1/2}$ and $p_{3/2}$ which have slightly different phases due to spin-orbit interaction. Their amplitudes therefore pass through zero at different energies that leads to a finite nonzero minimum value in the cross section. Position and magnitude of the minimum provides a sensitive probe of electron correlation and relativistic effects.

There are three measurements [1–3] available for comparison in this energy region. All three experimental measurements qualitatively agree with each other; however, the more recent measurements by Sander *et al.* [3] show a considerably lower minimum than those obtained in previous two experiments [1,2]. The measurements by Sander *et al.* [3] were designed especially for the study of the near-threshold region and we may consider them as benchmark data. The present calculation very well reproduced the experimental results at threshold. Our results also satisfactorily reproduce the magnitude of the minimum. The calculated position of minimum at 0.27 eV is slightly higher than the experimental position at 0.24 eV. Our calculation also shows that the inclusion of core polarization considerably shifts the minimum position from the DF value of 0.8 eV to lower energies and inclusion of the inner-core correlation shifts the minimum to higher energies. The final location of the minimum is a result of the interplay of these two main correlation effects. As seen from Fig. 3, there is only qualitative agreement with other theories. Nonrelativistic MCHF calculation by Saha [6] produces the minimum at a position of 0.2 eV, but he predicts a zero minimum due to the absence of spin-orbit interaction. The RMBPT calculation [8] shows the minimum too close to the threshold. The model-potential calculation [4] provides close agreement with experiment, but in this calculation one of the adjustable

parameters, a cutoff radius in the core-polarization term, was fitted to obtain the correct minimum position. The *ab initio* core-polarization calculations by Petrov *et al.* [7] (not shown in the Fig. 3 due to the lack of numerical data for the cross sections shown in their Fig. 2) also very accurately predict the minimum position at 0.23 eV, but their magnitude of minimum of 0.015 Mb is considerably lower than the experimental value of 0.035 Mb. Our cross section at the minimum is 0.028 Mb.

B. Photoionization of the excited states

Several results for photoionization of the 4p excited state are available in the literature. The photoionization cross sections of the 4p levels in K are shown in Fig. 4, where our results in DF and polarized-states approximations are compared with experimental measurements of Petrov *et al.* [10] and Amin *et al.* [11]. The comparison is also shown with the polarization potential calculation of Petrov *et al.* [10]. The effects of core polarization on near-threshold photoionization cross sections are expected to be less important for excited states because of less core penetration by the outer valence electron. However, Petrov *et al.* [10] noted strong deviation of the measured 4p cross sections from the theoretical prediction based on the Hartree-Fock approach. As seen from Fig. 4, the inclusion of core polarization is very important and it raises the photoionization cross section near threshold by more than a factor of 2. Theoretical cross sections obtained in different approximations converge to each other with increasing photon energy. Our results are in reasonable agreement with the experimental data and are about 10% lower than the calculated cross sections of Petrov *et al.* [10]. The experimental cross sections of Petrov *et al.* [10] were reported only for the laser-excited K(4$p_{3/2}$) level, whereas Amin *et al.* [11] reported the cross sections for both the 4$p_{3/2}$ and 4$p_{1/2}$ fine-structure levels
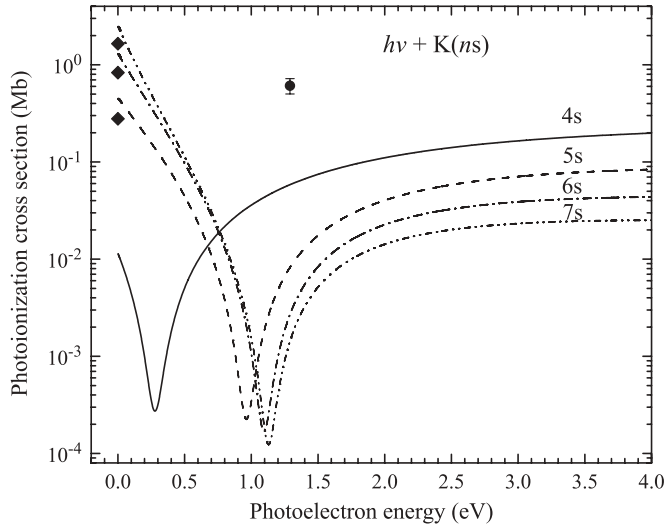
FIG. 5. Comparison of photoionization cross sections for ns ($n =$ 4–7) states of K as a function of photoelectron energy. Lines represent the present results; (solid diamonds) theoretical results of Aymar *et al.* [28] for threshold values of the $5s$, $6s$, and $7s$ photoionizations, which increase with n values; (solid circle) experimental data [11] for the $7s$ photoionization.

FIG. 6. Comparison of photoionization cross sections for nd ($n =$ 3–5) states of K as a function of photoelectron energy. Lines represent the present results; (solid diamonds) theoretical results of Aymar *et al.* [28] for threshold values of the $3d$, $4d$, and $5d$ photoionizations; (solid circle, triangle, and square) experimental data [11] for the $5d_{5/2}$, $5d_{3/2}$, and $5d_{5/2,3/2}$ photoionizations, respectively.

at selected laser wavelength of 355 nm. Their measured cross section of 7.2 Mb for $4p_{3/2}$ level is in excellent agreement with the previously measured value of 7.6 Mb by Burkhardt *et al.* [27] at the same laser wavelength. However, their cross section of 5.6 Mb for the $4p_{1/2}$ level differs considerably with the cross section for the $4p_{3/2}$ level. The cross sections for the $4p_{3/2}$ and $4p_{1/2}$ fine-structure levels may differ due to the influence of the spin-orbit splitting. Our results presented in Fig. 4 show a difference of only a few percentages between the $4p_{3/2}$ and $4p_{1/2}$ cross sections at all photon energies. The possible cause of large difference between cross sections for the $4p_{3/2}$ and $4p_{1/2}$ fine-structure levels found in Ref. [11] is not clear.

Even more striking differences are found between the present calculations and experimental data [11] for photoionization of the $7s$ and $5d$ excited levels in potassium. Figure 5 compares the photoinization cross sections for $4s$ ground and $5s$-$7s$ excited levels. All ns ($n = 4$–7) cross sections are similar in shape and exhibit the Cooper minimum which for excited states is shifted to higher energies in comparison to the $4s$ ground-state photoionization. The threshold photoionization cross sections monotonically increase, whereas the cross sections monotonically decrease at higher photoelectron energies with n values. Figure 5 reports the cross sections calculated with polarized pseudostates; however, the influence of core polarization quickly diminishes with increasing n value. For $7s$ photoionization, for example, the core polarization correction was found to be less than 1% at all photoelectron energies. There is only one experimental value available for comparison for photoionization of excited ns states in potassium. Amin *et al.* [11] employed two-photon resonance excitation process with laser wavelength of 660.6 nm, that correspond to photoelectron energy of 1.290 eV and reported the value of photoionization from the $7s$ $^2S_{1/2}$ state as $\sigma = 0.61 \pm 0.09$ Mb. As seen from Fig. 5, there is a huge difference of several orders between experiment and
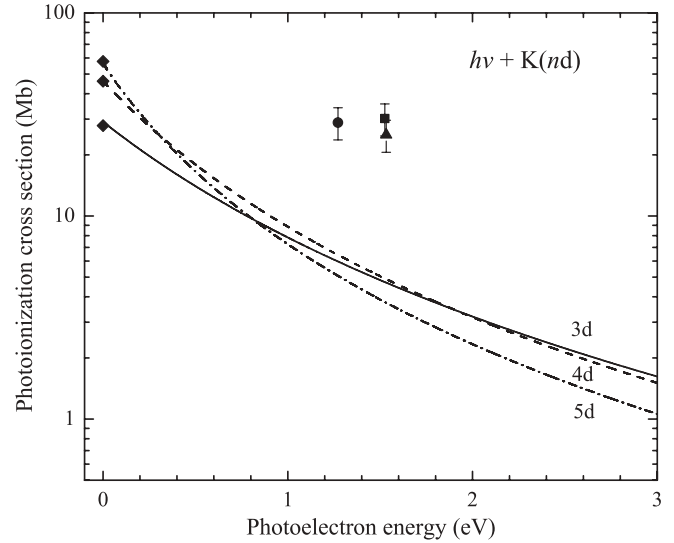
the present calculation at this energy point. Our calculations predict a Cooper minimum in this energy region with cross section of the order of 10^{-3} Mb, whereas the experimental cross section is closer to the threshold value of 2.35 Mb. The only other theoretical results available for comparison are the threshold cross sections for ns levels reported by Aymar *et al.* [28]. They used a single-particle central-field nonrelativistic model, and as seen from Fig. 5, their threshold values are in reasonable agreement with the present calculations.

Considerable difference between theory and experiment is also noted for the photoionization of the $5d$ excitation levels. The nd photoionization cross sections for the $3d$-$5d$ levels are presented in Fig. 6. Amin *et al.* [11] reported the $5d$ photoionization cross sections obtained in different ionization modes at three photoelectron energies of 1.871, 2.125, and 2.133 eV. The measured values of the cross sections from the $5d_{5/2}$ state by two-photon excitation from the ground state is 28.974.3 Mb, whereas in the two-step excitation, the cross section from the $5d_{3/2}$ state via the $4p_{1/2}$ state and from the $5d_{5/2,3/2}$ states via the $4p_{3/2}$ state are determined as 25.173.8 and 30.274.5 Mb, respectively. As seen from Fig. 6, all experimental values are close to each other but differ from the present predictions by up to a factor of 5. The calculated cross sections for nd states smoothly decrease from the maximum in the threshold energy region. Our cross sections at threshold energies agree very well with the single-particle calculations [28]. We also found that the nd photoionization cross sections are rather insensitive to the inclusion of polarized states and other correlation corrections. The reason of discrepancies with the experimental values [11] is not clear.

IV. CONCLUSIONS

In this article we presented new detailed calculations of the photoionization of potassium at low photon energies.

Photoionization of the $4s$ ground state and $4p$, $5s$-$7s$, and $3d$-$5d$ excited states of K have been considered. The present calculations were motivated partly by considerable diversity of the existing theoretical and experimental data for the ground-state photoionization and partly by appearance of new experimental data for photoionization from excited states which had no theoretical interpretation.

The calculations were carried out by using a fully relativistic Dirac B-spline R-matrix method [13]. In the present article we report the further extension of our DBSR complex by introducing polarized pseudostates as a complete and computationally efficient way to incorporate the core-valence correlation effects. Our approach differs from previous applications of polarized pseudostates by using nonorthogonal orbitals for the polarized wave functions and for the correlated orbitals used in the description of the inner-core correlation. It provides more flexibility in the applications and also may speed up the convergence of the configuration expansions.

The present calculations confirm that the core-valence correlation effects (core-polarization effects) have much influence on the photoionization of K from the $4s$ ground state. We also found that in addition to the dipole polarization, quadrupole polarization also should be taken into account and can lead to a correction of up to 10%. We accurately reproduce the position and magnitude of the near-threshold minimum based on *ab initio* calculations. Inclusion of the relativistic effects and inner-core correlation are also important. For higher energies, our $4s$ photoionization cross sections most closely agree with the measurements by Marr and Creek [2] and with the calculation of Petrov *et al.* [7].

The situation with photoionization of excited states is more complicated. Our calculations for the $4p_{3/2}$ cross section are in reasonable agreement with experimental and theoretical data presented in Ref. [8]. We obtained a very small difference between $4p_{3/2}$ and $4p_{1/2}$ photoionization cross sections, whereas a large difference was found in the measurements [11]. Even larger differences were found for $7s$ and $5d$ photoionization. Our calculations predict the deep minimum in the ns ($n = 5$–7) photoionization cross sections around 1 eV, whereas measured cross section [11] for the excited $7s$ state are larger by two orders of magnitude. Large discrepancies of up to a factor of 5 were also found with experiment [11] for the $5d$ photoionization. Theoretical photoionization cross sections of the nd levels show a very small dependence on the correlation effects. Large discrepancies with experiment [11] calls for additional measurements of the photoionization cross sections from the excited states of potassium.

[1] R. D. Hudson and V. L. Carter, Phys. Rev. **139**, A1426 (1965).

[2] G. V. Marr and D. M. Creek, Proc. R. Soc. A **304**, 233 (1968).

[3] W. Sandner, T. F. Gallagher, K. A. Safinya, and F. Gounand, Phys. Rev. A **23**, 2732 (1981).

[4] J. C. Weisheit, Phys. Rev. A **5**, 1621 (1972).

[5] M. G. J. Fink and W. R. Johnson, Phys. Rev. A **34**, 3754 (1986).

[6] H. P. Saha, Phys. Rev. A **39**, 628 (1989).

[7] I. D. Petrov, V. I. Sukhorukov, and H. Hotop, J. Phys. B **32**, 973 (1999).

[8] I. M. Savukov, Phys. Rev. A **76**, 032710 (2007).

[9] K. J. Niggard, R. E. Hebner, J. D. Jones, and R. J. Crbin, Phys. Rev. A **12**, 1440 (1975).

[10] I. D. Petrov, V. I. Sukhorukov, E. Leber, and H. Hotop, Eur. Phys J. D **10**, 53 (2000).

[11] N. Amin, S. Mahmood, S. U. Haq, M. A. Kalyar, M. Rafiq, and M. A. Baig, J. Quant. Spectrosc. Radiat. Transfer **109**, 863 (2008).

[12] O. Zatsarinny, Comput. Phys. Commun. **174**, 273 (2006).

[13] O. Zatsarinny and K. Bartschat, Phys. Rev. A **77**, 062701 (2008).

[14] O. Zatsarinny and K. Bartschat, Phys. Rev. A **79**, 042713 (2009).

[15] C. Froese Fischer and O. Zatsarinny, Comput. Phys. Commun. **180**, 879 (2009).

[16] P. Jönsson, X. He, C. Froese Fischer, and I. P. Grant, Comput. Phys. Commun. **177**, 597 (2007).

[17] R. J. Damburg and E. Karule, Proc. Phys. Soc. London **90**, 637 (1967).

[18] K. Bartschat, E. T. Hudson, M. P. Scott, P. G. Burke, and V. M. Burke, J. Phys. B **29**, 2875 (1996).

[19] I. Bray, D. V. Fursa, A. S. Kheifets, and A. T. Stelbovics, J. Phys. B **35**, R117 (2002).

[20] P. G. Burke and J. F. B. Mitchell, J. Phys. B **7**, 665 (1974).

[21] A. Hibbert, M. Le Dourneuf, and Vo Ky Lan, J. Phys. B **10**, 1015 (1977).

[22] P. H. Norrington and I. P. Grant, J. Phys. B **14**, L261 (1981).

[23] I. G. Young and P. H. Norrington, Comput. Phys. Commun. **83**, 215 (1994).

[24] M. A. Crees, Comput. Phys. Commun. **19**, 103 (1980).

[25] U. I. Safronova and M. S. Safronova, Phys. Rev. A **78**, 052504 (2008).

[26] M. J. Seaton, Proc. R. Soc. A **208**, 418 (1951).

[27] C. E. Burkhardt, J. L. Libbert, Jian Xu, J. J. Leventahl, and J. D. Kelley, Phys. Rev. A **38**, 5949 (1988).

[28] M. Aymar, E. Luc-Koenig E, and F. C. Farnoux, J. Phys. B **9**, 1279 (1976).

[29] U. Opik, Proc. Phys. Soc. London **92**, 566 (1967).

[30] W. R. Johnson, D. Kolb, and K. Huang, At. Data Nucl. Data Tables **28**, 333 (1983).

[31] I. S. Lim, J. K. Laerdahl, and P. Schwerdtfeger, J. Chem. Phys. **116**, 172 (2002).

[32] S. G. Porsev and A. Derevianenko, J. Chem. Phys. **119**, 844 (2003).